Homogenization of periodic elastic composites and locally resonant sonic materials

Sia Nemat-Nasser[a], John R. Willis[b], Ankit Srivastava[a], Alireza V. Amirkhizi[a]

[a] *Department of Mechanical and Aerospace Engineering*
University of California, San Diego, La Jolla, CA, 92037-0415
USA June 2010
[b] *Department of Applied Mathematics and Theoretical Physics*
Centre for Mathematical Sciences
Wilberforce Road, Cambridge CB3 0WA, UK

Abstract

A method for homogenization of an elastic composite with periodic microstructure is presented. It is shown that the resulting homogenized frequency-dependent elasticity and mass-density automatically satisfy the overall conservation laws and, independently, the dispersion relations that may also be calculated using other techniques, based on the microstructure of the associated unit cell. The method is used to calculate the effective parameters for a layered composite by using both the exact solution and the results of an approximate mixed variational formulation. The exact and approximate results are shown to be in close agreement which makes it possible to use the approximate method for homogenization in cases where an exact solution does not exist. The homogenized frequency-dependent effective parameters give rise to the concept of Dynamic Ashby charts that can be used to illustrate the effect of the micro-structural architecture on the dynamic properties of a composite. In particular, the charts vividly display how the effective stiffness and density vary with frequency and attain negative values within certain frequency ranges which can be changed as desired using the micro-architecture while keeping the volume fraction of the unit cell's constituents constant. Finally, an ambiguity in the nature of the optical branch of a 2-layered composite is discussed and a 4-layered composite is presented, which exhibits an unambiguously negative optical branch, for which the phase and group velocities are unambiguously antiparallel.

1 Introduction

There has been a recent surge of interest in the field of the dynamic response of composites with tailor-made microstructure. By controlling the micro-structural heterogeneities in a periodic composite, exotic dynamic responses at the macro

Preprint submitted to Elsevier *11 June 2010*

scale can be achieved. This necessitates developing systematic homogenization procedures by which the dynamic behavior of periodic composites may be expressed in terms of averaged parameters such as effective compliance and effective density. For wavelengths that are suitably larger than the scale of heterogeneity, these homogenized material parameters are expected to provide an effective description of the dynamic behavior of the composite. As a minimum, the resulting effective parameters must satisfy two basic conditions: (1) the overall conservation laws; and (2) the composite's dispersion relations. These dispersion relations can be accurately and independently calculated based on the microstructure of the unit cell, as we discuss in this paper.

For electromagnetic waves, Pendry and Smith [1–3] gave a method of homogenization of periodic composites using surface and line integrals of field variables. They pointed out that the effective parameters calculated from their method exhibit spatial dispersion for a homogeneous case and correct for this by removing the factor introduced by finite differencing of Maxwell's equations. Their method was applied to study chiral media by Amirkhizi and Nemat-Nasser [4]. The method we present in this paper does not require any such correction and in fact the corresponding results satisfy the above-mentioned two basic requirements exactly. Amirkhizi and Nemat-Nasser [5] have given a micro-structurally-based homogenization technique for calculating effective electromagnetic properties in which the values of the field variables in the unit cell are not required and that their results do satisfy the above-stated two basic requirements. Their 'Bloch' reduced form is in correspondence with the ensemble averaging technique proposed by Willis [6] who has applied it for calculating effective elastodynamic parameters for laminated media using Green's function. The effective parameters calculated from Willis' method satisfy the dispersion relation and are non-dispersive in the long wavelength limit. Here we present an analogous approach for calculating effective elastodynamic parameters ($C^{\text{eff}}, \rho^{\text{eff}}$) in periodic composites. This method is used to calculate the effective parameters for a 2-layered composite by using the exact solution given by Rytov [7] and an approximate mixed variational method proposed by Nemat-Nasser [8–10]. The efficacy and accuracy of the approximate method were demonstrated by means of numerical examples by Nemat-Nasser. Babuška and Osborn [11] subsequently proved the convergence of the method and that this convergence is an order faster than that of the usual Rayleigh quotient. Here we show, by way of a 2-layered example, that dispersion results obtained by using the approximate method quickly converge to the exact solution. The displacement and stress fields thus calculated from the approximate method are used to calculate the effective overall parameters and it is shown that the results converge to the results of the homogenization calculations based upon the exact solution. This is done with the view of subsequently using the approximate method to homogenize more complex composites where exact expressions for the field quantities and the dispersion relations do not exist.

The effective parameters, thus calculated, are functions of frequency. An efficient and logical way of representing them is by multi-dimensional graphs which we call Dynamic Ashby charts. These charts are extensions of the standard Ashby charts [12], in which the frequency (or wave vector) forms an additional axis. We illustrate how these charts may be used to tailor the effective dynamic properties of heterogeneous composites using architectural design of the microstructure. We show that, using the same volume fraction of constituents within a unit cell but varying the cell's micro-architecture, composites of vastly different dynamic properties can be created; e.g., composites with negative effective mass-density and/or negative effective stiffness, which may display negative index of refraction over a certain desired frequency range.

Veselago [13] in his paper on hypothetical materials with negative index of refraction showed that such materials, if realized, would possess exotic electromagnetic properties. These materials exhibit group velocity which is anti-parallel to phase velocity and were experimentally realized by Smith et. al. [14]. 'Negative' electromagnetic materials are a result of local substructural resonances in electric and magnetic fields. Analogous elastic materials with anti-parallel group velocity were proposed by Sheng et. al. [15], Liu et. al. [16], and Milton and Willis [17]. The central idea was to use local resonances from rigid body motions to create low frequency bands of negative group velocity. We present a 4-layered composite which uses this idea and exhibits a low frequency negative passband. The nature of the optical branch in the dispersion curve of a bi-layered composite, which may be considered a negative branch, is ambiguous and we present some comments regarding this issue. Our 4-layered composite, on the other hand, exhibits an unambiguous negative branch.

In what follows, we first present a general variational method that yields accurate eigenvalues and eigenmodes for periodic composites whose corresponding unit cell consists of constituents with discontinuous properties. Then we use the results to calculate the frequency-dependent effective stiffness and mass-density of a 2-layered composite, comparing the results with those based on the exact solution of the field equations. Finally, we present the concept of Dynamic Ashby chart and illustrate this for a 2-layered composite, demonstrating the effect of micro-structural design on the dynamic response of the composite.

2 Mixed method for calculation of eigenmodes of periodic composites

Consider harmonic waves in an unbounded periodic elastic composite consisting of a collection of unit cells, Ω. In view of periodicity, we have $\rho(\mathbf{x}) = \rho(\mathbf{x}+m^{'}I^{\beta})$, and $C_{jkmn}(\mathbf{x}) = C_{jkmn}(\mathbf{x}+m^{'}I^{\beta})$, where $\mathbf{x}$ is the position vector with components $x_j, j = 1, 2, 3$, $\rho(\mathbf{x})$ is the density and $C_{jkmn}(\mathbf{x}), (j, k, m, n = 1, 2, 3)$ are the components of the elasticity tensor in Cartesian coordinates. m' is any integer and $I^\beta, \beta = 1, 2, 3$, denote the three vectors which form a parallelepiped enclosing the periodic unit cell.

For time harmonic waves with frequency ω ($\lambda = \omega^2$), the field quantities are proportional to $e^{\pm i\omega t}$. The field equations become,

$$\sigma_{jk,k} + \lambda\rho u_j = 0; \quad \sigma_{jk} = C_{jkmn}u_{m,n} \tag{1}$$

For harmonic waves with wavevector $\mathbf{q}$, the Bloch boundary conditions take the form,

$$u_j(\mathbf{x} + I^\beta) = u_j(\mathbf{x})e^{i\mathbf{q}.I^\beta}; \quad t_j(\mathbf{x} + I^\beta) = -t_j(\mathbf{x})e^{i\mathbf{q}.I^\beta} \tag{2}$$

for $\mathbf{x}$ on $\partial\Omega$, where $\mathbf{t}$ is the traction vector.

To find an approximate solution of the field equations (Eq. 1) subject to the boundary conditions (Eq. 2), we consider the following estimates:

$$\bar{u}_j = \sum_{\alpha,\beta,\gamma=-M}^{+M} U_j^{(\alpha\beta\gamma)} f^{(\alpha\beta\gamma)}(\mathbf{x}) \tag{3}$$

$$\bar{\sigma}_{jk} = \sum_{\alpha,\beta,\gamma=-M}^{+M} S_{jk}^{(\alpha\beta\gamma)} f^{(\alpha\beta\gamma)}(\mathbf{x}) \tag{4}$$

where the approximating functions $f^{(\alpha\beta\gamma)}$ are continuous and continuously differentiable, satisfying the Bloch periodicity conditions. As shown by Nemat-Nasser, the eigenvalues are obtained by rendering the following functional stationary:

$$\lambda_N = (\langle\sigma_{jk}, u_{j,k}\rangle + \langle u_{j,k}, \sigma_{jk}\rangle - \langle D_{jkmn}\sigma_{jk}, \sigma_{mn}\rangle)/\langle\rho u_j, u_j\rangle \tag{5}$$

where $\langle gu_j, v_j\rangle = \int_\Omega gu_jv_j^*\mathrm{dV}$ and D_{jkmn} are the components of the elastic compliance tensor, the inverse of the elasticity tensor C_{jkmn}.

Substituting Eq. (3, 4) into Eq. (5) and equating to zero the derivatives of λ_N with respect to the unknown coefficients $U_j^{(\alpha\beta\gamma)}$ and $S_{jk}^{(\alpha\beta\gamma)}$, we arrive at the following set of linear homogeneous equations:

$$\langle\bar{\sigma}_{jk,k} + \lambda_N\rho\bar{u}_j, f^{(\alpha\beta\gamma)}\rangle = 0;\ ^{1} \quad \langle D_{jkmn}\bar{\sigma}_{mn} - \bar{u}_{j,k}, f^{(\alpha\beta\gamma)}\rangle = 0\ ^{2} \tag{6}$$

There are $6M_p^3$ ($M_p = 2M+1$) equations in Eq. $(6)^2$ for a general 3-directionally periodic composite. They may be solved for $S_{jk}^{(\alpha\beta\gamma)}$ in terms of $U_j^{(\alpha\beta\gamma)}$ and the result substituted into Eq. $(6)^1$. This leads to a system of $3M_p^3$ linear equations. The roots of the determinant of these equations give estimates of the first $3M_p^3$ eigenvalue frequencies. The corresponding eigenvectors are $U_j^{(\alpha\beta\gamma)}$ from which the displacement field within the unit cell is reconstituted. The stress variation in the unit cell is obtained from Eq. $(6)^2$. The following example illustrates this procedure; as has been proved by Babuška and Osborn [11], the results converge at a rate that is an order of magnitude faster than that of the Rayleigh quotient.

2.1 Example: A layered composite

To evaluate the effectiveness of the mixed variational method, consider a layered composite (Fig. 1) with harmonic waves traveling perpendicular to the layers. The displacement, u, and stress, σ, are approximated by,

$$\bar{u} = \sum_{\alpha=-M}^{+M} U^{(\alpha)} e^{i(qx+2\pi\alpha x/a)}; \quad \bar{\sigma} = \sum_{\alpha=-M}^{+M} S^{(\alpha)} e^{i(qx+2\pi\alpha x/a)} \tag{7}$$

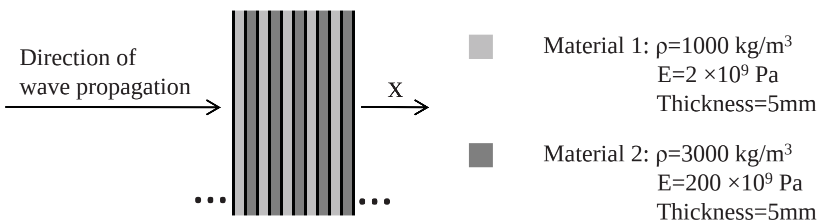

Fig. 1. Schematic of a layered composite

Substituting the above into Eq. $(6)^2$ we obtain S^α in terms of U^α. The resulting equations are then substituted into Eq. $(6)^2$, providing a set of M_p linear homogeneous equations, the roots of whose determinant give the first M_p eigenvalue frequencies for a given wavenumber q. In Fig. (2) we compare the frequency-wavenumber dispersion relations obtained by this mixed variational method and the exact solution [7].

The first four modes are compared in Fig. (2). It can be seen that the mixed method gives accurate results for the first three modes when $M_p = 5(M = 2)$ terms are used to approximate the displacement and stress. The fourth mode is inaccurate for the $M = 2$ calculation but as the number of terms in the expansion are increased to $M_p = 7(M = 3)$, the results converge to those obtained from the exact solution.

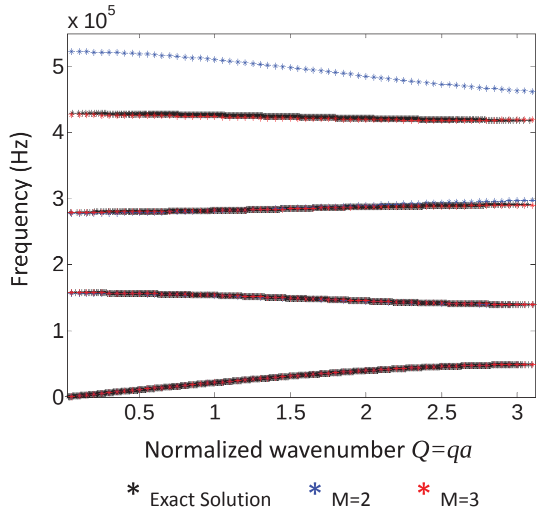

Fig. 2. Frequency-wavenumber dispersion relations; comparison of approximate and exact results

Since the exact dispersion relations are available for only fairly simple geometries like layered composites, the mixed variational formulation provides an attractive and effective method to calculate the eigenfrequencies and eigenvectors associated with the three-dimensionally periodic composites. In what follows, it will be shown that homogenization of layered composites based on the mixed variational formulation gives results which are very close to the exact-solution based homogenization, suggesting that the mixed variational method may be used for field-integral-based homogenization in cases where the exact solution does not exist.

3 Homogenization by integration of field variables

For harmonic waves traveling in a layered composite with a periodic unit cell $\Omega = \{x : -a/2 \leq x < a/2\}$ the field variables (displacement, velocity, stress, and momentum) take the following Bloch form,

$$u(x,t) = U(x)e^{i(qx-\omega t)}; \quad v(x,t) = -i\omega U(x)e^{i(qx-\omega t)} \tag{8}$$

$$\sigma(x,t) = \Sigma(x)e^{i(qx-\omega t)}; \quad p(x,t) = \rho(x)v(x,t) = P(x)e^{i(qx-\omega t)} \tag{9}$$

where functions $U(x)$, $\Sigma(x)$, and $P(x)$ are periodic with the periodicity of the unit cell. The dynamic equilibrium gives,

$$\nabla\sigma + i\omega p = 0 \tag{10}$$

where ∇ denotes differentiation with respect to x.

4 Effective properties

Multiply Eq. (10) by e^{-iqX} and use Eqs. (8, 9) to obtain,

$$\nabla \left(\Sigma(x) e^{iq(x-X)} \right) + i\omega P(x) e^{iq(x-X)} = 0 \tag{11}$$

Introduce the change of variable $y = x - X$ to obtain,

$$\nabla_y \left(\Sigma(X+y) e^{iqy} \right) + i\omega P(X+y) e^{iqy} = 0 \tag{12}$$

Average the above equation with respect to X over the unit cell, to arrive at,

$$\nabla_y \left(\bar{\Sigma} e^{iqy} \right) + i\omega \bar{P} e^{iqy} = 0 \tag{13}$$

where

$$\bar{\Sigma} = \frac{1}{2L} \int_{-L}^{+L} \Sigma(x) dx; \quad \bar{P} = \frac{1}{2L} \int_{-L}^{+L} P(x) dx \tag{14}$$

Now define the *mean stress* and *mean momentum density* as,

$$\langle \sigma \rangle (x) = \bar{\Sigma} e^{iqx}; \quad \langle p \rangle (x) = \bar{P} e^{iqx} \tag{15}$$

Observe that the mean stress and mean momentum density satisfy exactly the overall equation of motion,

$$\nabla \langle \sigma \rangle + i\omega \langle p \rangle = 0 \tag{16}$$

Define the effective mean displacement as,

$$\langle u \rangle (x) = \bar{U} e^{iqx}; \quad \bar{U} = \frac{1}{2L} \int_{-L}^{+L} U(x) dx \tag{17}$$

Then the effective mean strain and velocity are given by,

$$\langle e\rangle(x) = iq\langle u\rangle(x); \quad \langle v\rangle(x) = -i\omega\langle u\rangle(x) \tag{18}$$

Finally, the averaged stress-strain relation becomes,

$$\langle\sigma\rangle(x) = C^{\text{eff}}\langle e\rangle(x) \tag{19}$$

Based on Eq. (15, 18), C^{eff} is given by,

$$C^{\text{eff}} = \frac{\bar{\Sigma}}{iq\bar{U}} \tag{20}$$

Similarly, the effective density (ρ^{eff}) is given by,

$$\rho^{\text{eff}} = \frac{\bar{P}}{-i\omega\bar{U}} \tag{21}$$

Since $\langle\sigma\rangle$ and $\langle p\rangle$ satisfy the equation of motion (Eq. 16), it is seen that the effective material parameters defined above automatically satisfy the dispersion relation,

$$\frac{C^{\text{eff}}}{\rho^{\text{eff}}} = \frac{\omega^2}{q^2} \tag{22}$$

We emphasize that, in this homogenization procedure due to Willis [6], the exact dispersion relations automatically emerge as results.

5 Homogenization of layered composites

To illustrate the above method of homogenization, the numerical example of Fig. (1) is considered again. Since the exact solution in the form of dispersion relation and displacement and stress fields exists for this simple layered case, it will be shown by way of comparison that results of the homogenization based upon the approximate mixed variational formulation rapidly converge to those based upon the exact solution, suggesting that the approximate method may be confidently used to estimate effective properties of 2- and 3- dimensionally periodic composites for which exact solutions cannot be constructed.

The exact dispersion relation for 1-D longitudinal wave propagation in a periodic layered composite has been given by Rytov [7],

$$\cos(qa) = \cos(\omega h_1/c_1)\cos(\omega h_2/c_2) - \Gamma \sin(\omega h_1/c_1)\sin(\omega h_2/c_2) \qquad (23)$$

$$\Gamma = (1+\kappa^2)/(2\kappa); \quad \kappa = \rho_1 c_1/(\rho_2 c_2) \qquad (24)$$

where h_i is the thickness, ρ_i is the density, and c_i is the longitudinal wave velocity of the i^{th} layer $(i = 1, 2)$ in a unit cell. Fig. (2) shows the dispersion curves corresponding to the first four propagating branches, for the layered composite shown in Fig. (1). These are calculated using the exact solution and the mixed variational formulation. For the frequency band corresponding to each of these branches, Eq. (23) yields real (normalized) wavenumbers $(0 \leq Q = qa \leq \pi)$ and a wave at a corresponding frequency travels undamped through the composite. Frequency bands within which no propagating mode exists constitute the stopbands. The normalized wavenumbers satisfying Eq. (23) for these frequencies take on the form $Q = \pi - i\alpha$ or $Q = i\alpha$, where α is a positive real number. These modes are non-propagating and their energy is trapped within the first few layers due to multiple reflections. As a result, the amplitude of a non-propagating wave decreases exponentially with propagation distance. Although an infinite number of propagating branches exist as the frequency under consideration is increased, meaningful homogenization can be carried out only for low frequency branches, below the refraction limit. Therefore, only the first two propagating branches are considered in what follows.

Fig. (3) shows the effective parameters calculated from Eqs. (20, 21) for the case of the 2 layered composite. Black curves in Figs. (3a,b) correspond to effective properties calculated from the exact solution whereas the red and blue curves are effective property calculations from the approximate mixed variational formulation for $M = 1, 2$ respectively. It can be seen that the homogenization results from the approximate method are in very good agreement with those from the exact solution. Fig. (3a) shows the variation of the effective density, and Fig. (3b) that of the effective compliance ($D^{\text{eff}} = 1/C^{\text{eff}}$) of the composite, as functions of frequency. It can be seen that the effective density and compliance are nearly constant for low frequencies and are equal to the volume average of those of the individual constituents of the unit cell. This is expected since at low frequencies the Bloch wavelength is much larger than the thickness of individual layers and the response of the composite is nearly static. Fig. (3c) shows the dispersion curves, based on the calculated effective parameters ($Q = a(\omega^2 \rho^{\text{eff}} D^{\text{eff}})^{1/2}$). It can be seen from Fig. (3c) that the calculated effective parameters exactly satisfy the dispersion relation of Fig. (2).

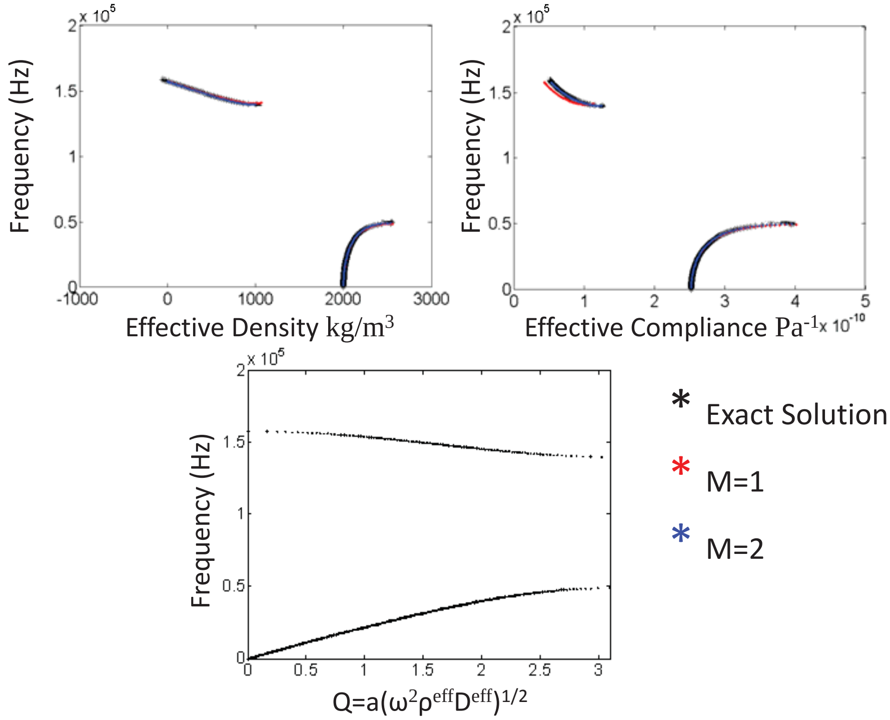

Fig. 3. Effective Parameters for layered composite: a. Effective Density (ρ^{eff}); b. Effective Compliance (D^{eff}); and c. Dispersion curve calculated from effective parameters

5.1 Dynamic Ashby chart representation

The effective material properties calculated above define propagation, reflection, and refraction of stress waves in the composite. They may be nicely dislayed in a 3-dimensional chart, as shown in Fig. 4. We refer to this kind of charts as generalized Dynamic Ashby charts. In general, Dynamic Ashby charts are obtained from the corresponding static ones (associated with zero frequency), augmented with additional axes (representing frequency and wavevector) that account for the dynamic effects on the material properties.

In Fig. 4, the 3-D trajectory (black spheres) shows the effective density and compliance as functions of frequency. Its projection on the $y - z$ plane (green curve) and $x - z$ plane (blue curve), respectively shows the variation of the effective compliance and density with the wave frequency.

5.2 Micro-architectural control of dynamic properties

In a standard Ashby chart the composite is represented by a single point that corresponds to its considered quasi-static properties. The effective dynamic

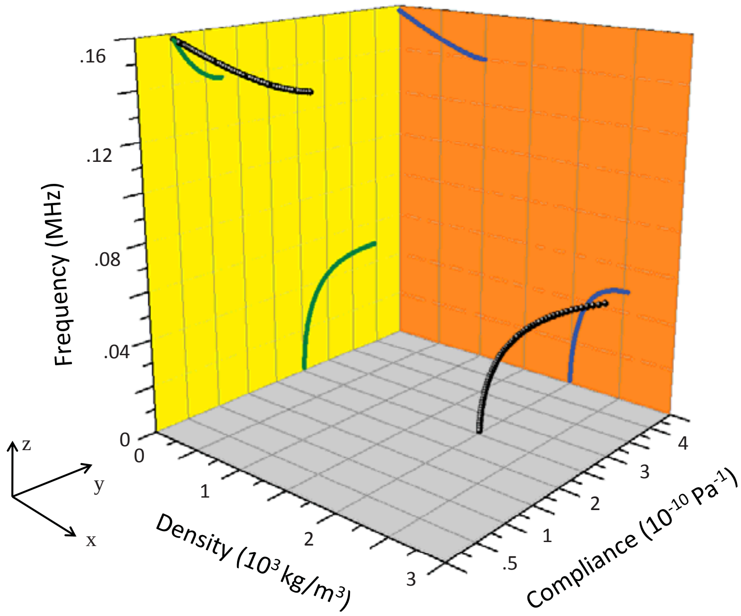

Fig. 4. Dynamic Ashby chart representation of frequency-dependent effective compliance and density.

properties of the composite however, can take on a broad range of values depending on its micro-architecture, that is, depending on the manner by which the composite's constituents are distributed within its unit cell. This is illustrated by comparing the dynamic trajectories of three simple architectures shown in Fig. (5) with the same static overall mass-density and compliance, i.e., all three trajectories start from the same point in the corresponding standard Ashby chart.

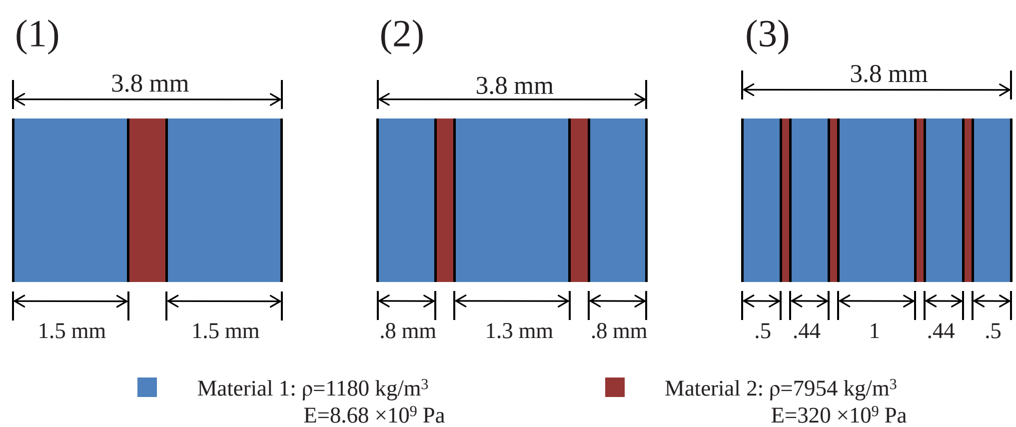

Fig. 5. Schematic of the architectures used for comparison

Starting with the same amount of each of the two materials per unit length, we consider the dynamic effects of their distribution within a unit cell according to three different architectures, denoted as (1), (2), and (3) in Fig. (5).

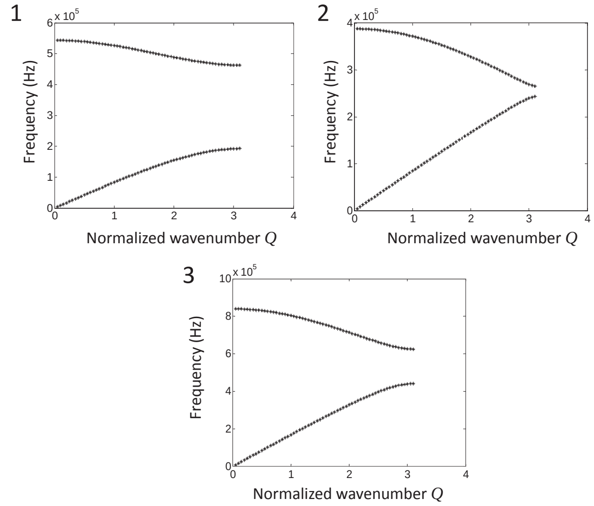

Fig. 6. Dispersion curves for considered micro-architectures.

Fig. (6) shows the dispersion curves for the first two propagating branches for the three cases. As material is redistributed from case (1) to case (2), the low-frequency stopband is decreased. For architecture (3) with a finer distribution of the two constituent materials, the overall dynamic response corresponds to higher frequencies as compared to those of the first two architectures.

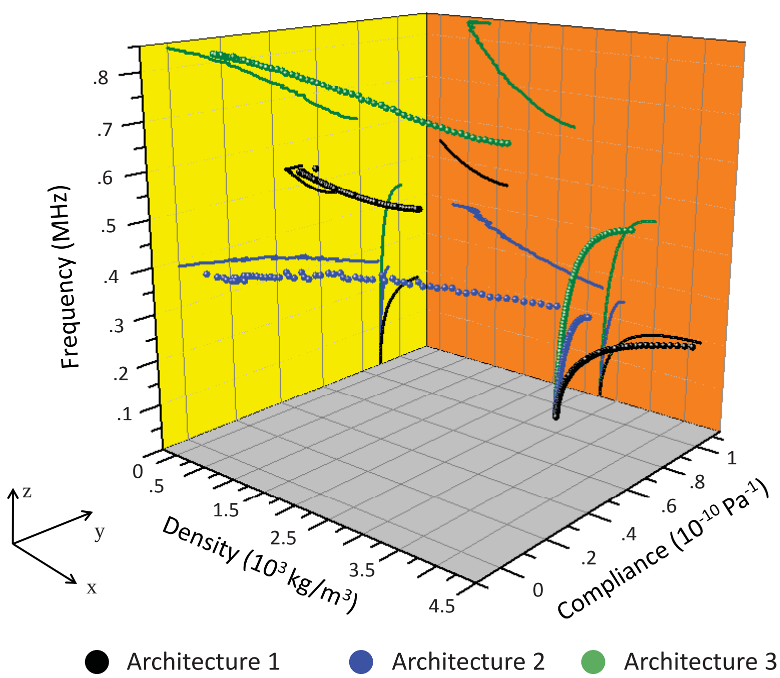

Fig. 7. Dynamic Ashby chart: effect of micro-architecture on dynamic properties.

Fig. (7) shows the corresponding trajectories for the three architectures in the Dynamic Ashby chart. All three trajectories start at the same point on the zero-frequency plane, with effective density $= 2742\ kg/m^3$ and effective compliance $= 8.94\times10^{-11}\ Pa^{-1}$, calculated according to the volume fraction of the constituents. It can be seen that the trajectories of effective density and compliance for the three architectures pass through significantly different regions within this 3-dimensional Dynamic Ashby chart. By changing the distribution scale of the individual constituent materials, it is seen that Architecture 3 exhibits a relatively static response at frequencies, up to about 300 kHz, but its dynamic response is frequency-dependent at higher frequencies. This illustrates how one can change the architecture at nano-, micro-, meso-, and macro-scales to manage stress waves over many windows of frequencies.

6 Locally resonant sonic composite

The dispersion relation for a 1-D, 2-layered composite for longitudinal Bloch wave propagation is given in Eq. (23). For a given frequency ω, there are infinite wavenumbers that satisfy this equation. For a non-dispersive homogeneous material, there are no band gaps, and the correct normalized wavenumber solution (Q') along the second branch is $Q' = 2\pi - Q$, where Q is the Bloch solution. For a layered heterogeneous composite, while the Bloch condition gives a normalized wavenumber solution between 0 and π its interpretation as negative branch may be ambiguous.

For the case of a 2-layered heterogeneous composite (Fig. 2) the second (optical) branch in the Bloch dispersion is considered a negative branch when the group velocity ($d\omega/dq$) for this branch is anti-parallel to its phase velocity (ω/q). If artificial folding has indeed occurred through the application of the Bloch constraint, the negative characteristic of the optical branch may not necessarily correspond to a negative branch. For Bloch wave propagation in layered composite, waves traveling in the positive and negative x direction exist in each layer. The actual wavenumber is equal to the phase advance through the unit cell, of either the positive wave (ϕ_P) or the negative wave (ϕ_N). This is possible because ϕ_P and ϕ_N are always separated by $2n\pi$ where n is a whole number. It is seen that for a 2-layered composite an ambiguity always exists ($\phi_P \neq \phi_N$) for the optical branch. We now present a 4-layered composite where there is no such ambiguity.

6.1 4-layered composite

We present a 4-layered case where there is no ambiguity that the optical branch is a negative branch. This happens when a heavy and stiff material is placed between thin layers of soft and light material and the whole assembly is in a heavy and stiff matrix.The case is similar to Sheng et. al. [15], Liu et. al. [16]

and Milton and Willis [17] and the idea is to use localized resonance of the rigid body motion of the heavy central layer to create bands of negative group velocity.

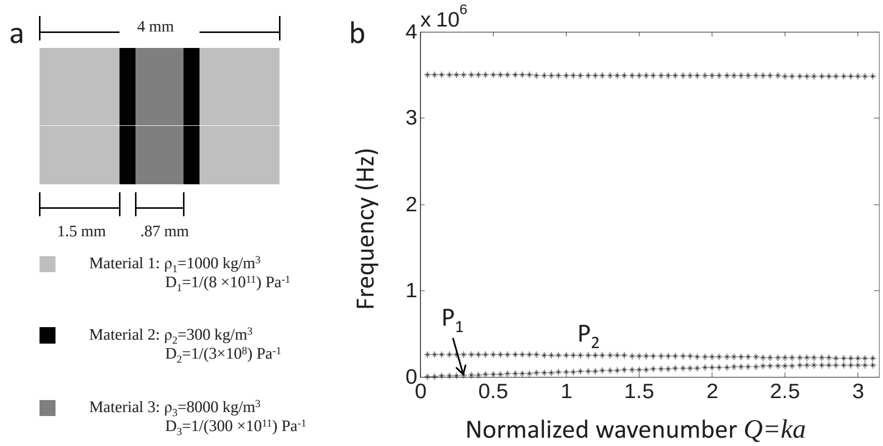

Fig. 8. 4 layered composite: a. Schematic of a unit cell; and b. Frequency-wavenumber dispersion curve.

Fig. (8a) shows the schematic diagram of a unit cell of the 4-layered composite considered. Fig. (8b) shows the dispersion curve for the composite. The first two propagating modes have been pushed to low frequencies and a significant stopband exists between the second and the third passbands. Fig. (9) shows the real part of the displacement profile along the unit cell at $Q = .5$ on branch P_2. It can be seen that there is a rigid body motion of the central layer with respect to the matrix. This gives rise to a local resonance and for this case $\phi_P = \phi_N = Q$ for the optical branch and there is no ambiguity that the optical branch is a negative branch.

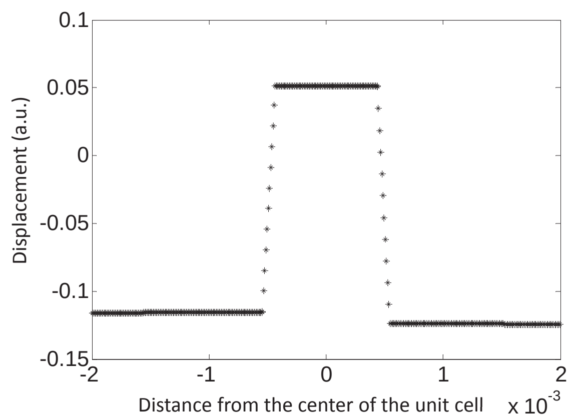

Fig. 9. Displacement profile along the unit cell at Q=.5, f=25.8 kHz.

7 Conclusions

A homogenization method, originally proposed by Willis [6] based on the integration of field variables over a unit cell, is presented. It is used to calculate the effective properties of a 2-layered composite, using both the exact solution and an approximate solution originally proposed by Nemat-Nasser [8] using a mixed variational formulation. It is shown that the effective parameters calculated from the approximate method quickly converge to the homogenization results based upon the exact solution. The effective parameters thus calculated are shown to satisfy the dispersion relation for the medium and are non-dispersive in the long wavelength limit. The results are presented in the context of Ashby-type charts, referred to as Dynamic Ashby charts, that provide an effective tool for the representation of frequency-dependent dynamic effective properties of composites. Finally we have mentioned that the nature of the optical branch in a bi-layered composite is ambiguous and presented a 4-layered composite which uses local resonance to produce an unambiguously negative optical branch.

8 Acknowledgement

This research has been conducted at the Center of Excellence for Advanced Materials (CEAM) at the University of California, San Diego. This work has been supported by DARPA AFOSR Grant FA9550-09-1-0709 to the University of California, San Diego.

References

[1] J.B. Pendry, Photonic band structures, *J. Mod. Opt.*, **41** (1994), pp. 209-229.

[2] J.B. Pendry, Calculating photonic band structure, *J. Phys.: Condens. Matter*, **8** (1996), pp. 1085-1108.

[3] D.R. Smith and J.B. Pendry, Homogenization of metamaterials by field averaging, *J. Opt. Soc. Am. B*, **23** (2006), pp. 391-403.

[4] A.V. Amirkhizi, S. Nemat-Nasser, Numerical calculation of electromagnetic properties including chirality parameters for uniaxial bianisotropic media, *Smart Mater. Struct.*, **17** (2008).

[5] A.V. Amirkhizi, S. Nemat-Nasser, Microstructurally-based homogenization of electromagnetic properties of periodic media, *Comptes Rendus Mecanique*, **336** (2007), pp. 24-33.

[6] J.R. Willis, Exact effective relations for dynamics of a laminated body, *Mechanics of Materials*, **41** (2009), pp. 385-393.

[7] S.M. Rytov, Acoustical properties of a thinly laminated medium, *Sov. Phys. Acoust.*, **2** (1956), pp. 6880.

[8] S. Nemat-Nasser, General variational methods for elastic waves in composites, *J. Elasticity*, **2** (1972), pp. 73-90.

[9] S. Nemat-Nasser, F.C.L. Fu, S. Minagawa, Harmonic waves in one-, two-, and three-dimensional composites: bounds for eigenfrequencies, *Int. J. of Solids and Struct.*, **11** (1975), pp. 617.

[10] S. Minagawa, S. Nemat-Nasser, Harmonic waves in three-dimensional elastic composites, *Int. J. of Solids and Struct*, **12** (1976), pp. 769-777.

[11] I. Babuška, J.E. Osborn, Numerical treatment of eigenvalue problems for differential equations with discontinuous coefficients, *Mathematics of Computation*, **32** (1978).

[12] M.F. Ashby, Materials selection in mechanical design, Butterworth-Heinemann Pub., (2005).

[13] V.G. Veselago, The electrodynamics of substances with simultaneously negative values of ε and μ, *Physics-Uspekhi*, **10** (1968), pp. 509-514.

[14] D.R. Smith, W.J. Padilla, D.C. Vier, S.C. Nemat-Nasser, S. Schultz, Composite medium with simultaneously negative permeability and permittivity, *Physical Review Letters*, **84** (2000), pp. 418-4187.

[15] P. Sheng, X.X. Zhang, Z. Liu, C.T. Chan, Locally resonant sonic materials, *Phys. B. Condens. Matter.*, **338** (2003), pp. 201-205.

[16] Z. Liu, C.T. Chan, P. Sheng, Analytic model of phononic crystals with local resonances, *Phys. Rev. B.*, **71** (2005), pp. 014-103.

[17] G.W. Milton, J.R. Willis, On modifications of Newton's second law and linear continuum elastodynamics, *Proceedings of the Royal Society A: Mathematical, Physical and Engineering Science*, **463** (2007), pp. 855-880.